Pure Appl. Chem., Vol. 80, No. 3, pp. 447–457, 2008.
doi:10.1351/pac200880030447

Disilyne with a silicon–silicon triple bond: A new entry to multiple bond chemistry*

Akira Sekiguchi

Department of Chemistry, Graduate School of Pure and Applied Sciences, University of Tsukuba, Tsukuba, Ibaraki 305-8571, Japan

Abstract: The synthesis, crystal structure, and characterization of a silicon–silicon triply bonded species, disilyne with two bis[bis(trimethylsilyl)methyl]isopropylsilyl substituents, are described. The nature of the sp-hybridized silicon atoms is discussed from the viewpoint of spectroscopic results and theoretical calculations. The reactivity of the disilyne with alkali metals, ^{t}BuLi, and π-bonded compounds such as *cis*- and *trans*-2-butenes and phenylacetylene is also described.

Keywords: aromaticity; disilabenzene; disilyne; main group 14 elements; multiple bond chemistry.

INTRODUCTION

Hydrocarbons containing >C=C< double and –C≡C– triple bonds, alkenes, and alkynes, respectively, form an abundant and structurally diverse class in organic chemistry. However, the ability of heavier congeners of carbon (E = Si, Ge, Sn, and Pb) to form multiple bonds of the type >E=E< and –E≡E– was doubted for a long time [1]. However, almost every type of doubly bonded compound having not only homo- and heteronuclear double bonds between group 14 elements of >E=E'< type (E and E' = C, Si, Ge, Sn, and Pb), but also double bonds between the heavier group 14 elements and other main group elements (groups 13, 15, and 16) have been synthesized and structurally characterized [1], since the discovery of the stable distannene $Dsi_2Sn=SnDsi_2$ (Dsi = $CH(SiMe_3)_2$) by Lappert in 1973 [2], tetramesityldisilene $Mes_2Si=SiMes_2$ (Mes = 2,4,6-trimethylphenyl) by West in 1981 [3], and $(Me_3Si)_2Si=C(OSiMe_3)Ad$ (Ad = 1-adamantyl) by Brook in 1981 [4]. Despite extensive experimental efforts directed toward the synthesis of triply bonded compounds of heavier group 14 elements, heavier analogs of alkynes, such as –E≡C– and –E≡E– (E = Si, Ge, Sn, and Pb), remained unknown until recently [5]. In 2000, Power reported the synthesis and structural characterization of the lead analog of the alkyne analogs [6], and subsequently, tin [7] and germanium [8] analogs were also synthesized by the same group in 2002 by using bulky terphenyl ligands (2,6-diarylphenyl groups) and by Tokitoh using the Bbt group {C_6H_2-2,6-[$CH(SiMe_3)_2$-4-$C(SiMe_3)_3$]}. However, the chemistry of disilyne with a silicon–silicon triple bond was missing until reports in 2004 by our group and Wiberg [9,10]. We present here the synthesis and structural characterization of a disilyne with a new type of π bond, as well as its reactivity [9,11].

*Paper based on a presentation at the 12th International Symposium on Novel Aromatic Compounds (ISNA-12), 22–27 July 2007, Awaji Island, Japan. Other presentations are published in this issue, pp. 411–667.

SYNTHESIS OF A DISILYNE

Based on both the theoretical prediction [12] and our previous experimental study [13], we have designed the $Dsi_2{}^iPrSi$ group [Dsi = $CH(SiMe_3)_2$] for the protection of a silicon–silicon triple bond. Disilyne **2** was prepared by reduction of the tetrabrominated precursor **1**. Thus, the reaction of **1** with four equivalents of potassium graphite (KC_8) in tetrahydrofuran (THF) produced a dark green mixture, from which disilyne **2** was isolated as extremely air- and moisture-sensitive emerald green crystals in 73 % isolated yield (Scheme 1) [9].

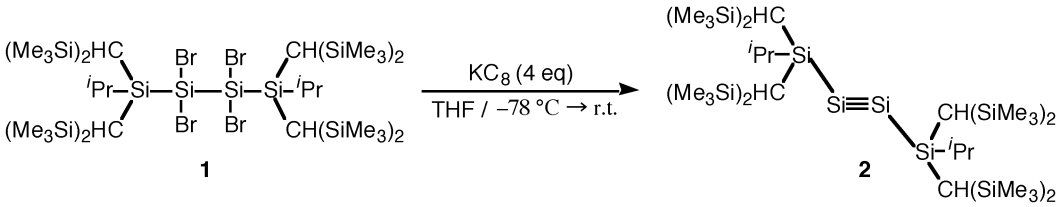

Scheme 1

Figure 1 shows the molecular structure of disilyne **2**. The four Si atoms (Si2, Si1, Si1', and Si2') are coplanar, and the bulky $Si^iPr[(CH(SiMe_3)_2]_2$ groups protect the central Si≡Si triple bond. The most significant result is the Si≡Si triple bond length of 2.0622(9) Å. This value is 3.8 % shorter than the typical Si=Si double bond length (2.14 Å) and 13.5 % shorter than the average Si–Si single bond length of 2.34 Å [1g]. This shortening is half the magnitude of that in the carbon counterparts. Moreover, alkynes have a linear geometry around the C≡C triple bond, whereas disilyne has the *trans*-bent geometry with a bending angle of 137.44(4)° around the Si≡Si triple bond. The structure of **2** presented here is close to that predicted by a density functional (DFT) calculation on $(^tBu_3Si)_2MeSiSi{\equiv}SiSiMe(Si^tBu_3)_2$ [14]. The space-filling model of **2** shown in Fig. 2 highlights the steric protection of the Si≡Si group by the isopropyl and bis(trimethylsilyl)methyl substituents. A DFT calculation on disilyne **2** at the B3LYP/6-31G(d) level of theory well reproduces the experimental geometry and the structural parameters (calculated value: 2.093 Å for the Si≡Si bond length, 136.1° for the *trans*-bending angle).

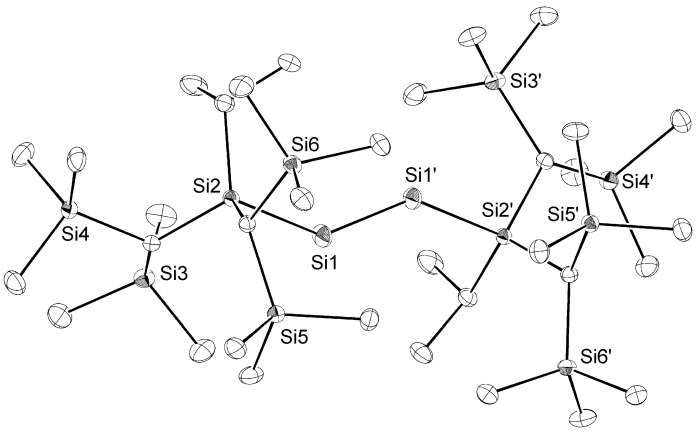

Fig. 1 ORTEP drawing of disilyne **2**.

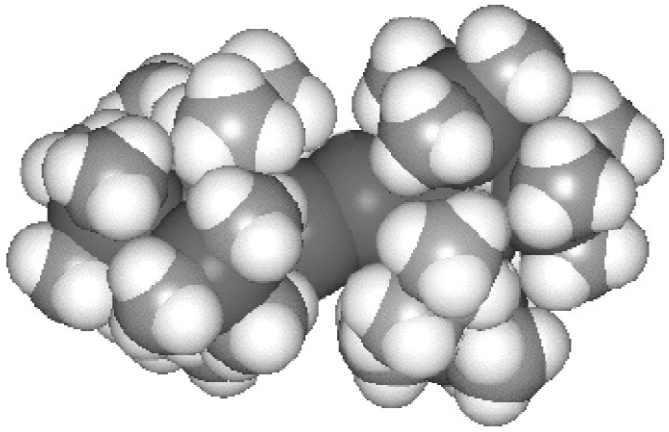

Fig. 2 Space filing model of disilyne **2**.

The bending is thought to be the result of the mixing of an in-plane π orbital with a σ* orbital whose energies are close enough to cause the interaction of these orbitals in the heavier elements (Fig. 3) [5e]. The σ orbital of the C–C bond cannot interact with an in-plane π orbital because of the large energy difference, whereas the Si–Si σ* orbital can interact with the in-plane π orbital to produce the *trans*-bent structure of RSi≡SiR {R = Si^{i}Pr[CH(SiMe$_3$)$_2$]$_2$}, resulting in a bond order of 2.618 [9].

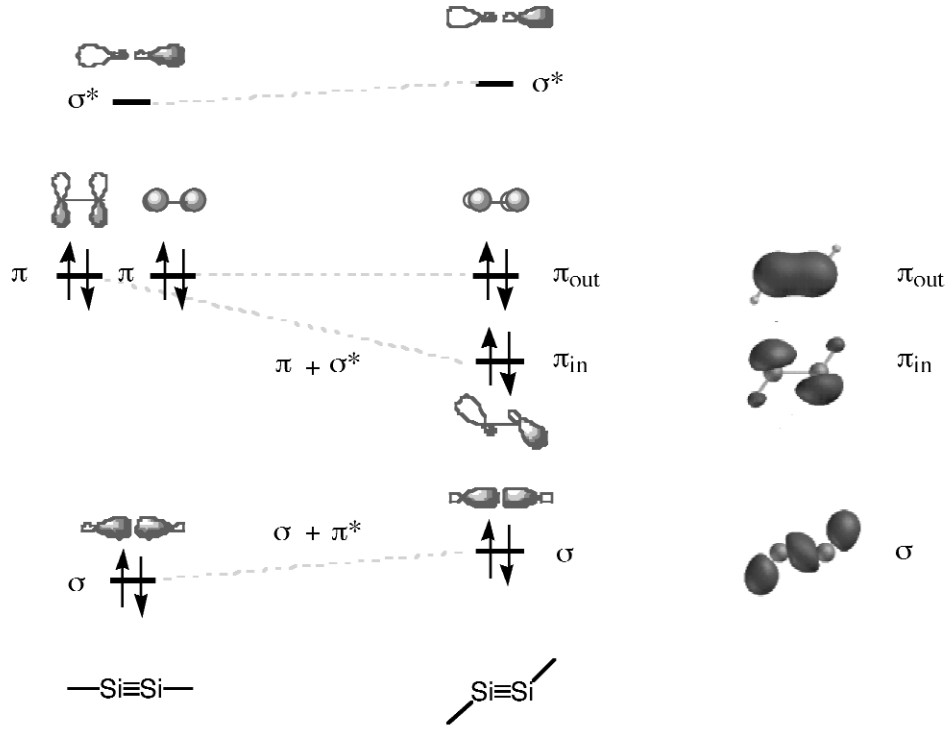

Fig. 3 Schematic MO diagrams of linear and *trans*-bent disilynes.

The molecular orbitals (MOs) of disilyne **2** calculated at the HF/6-311G(d)//B3LYP/6-31G(d) level presented in Fig. 4 show two nondegenerate highest occupied π MOs (HOMO–1 and HOMO) and two lowest unoccupied antibonding π* MOs (LUMO and LUMO+1) [9,15]. The out-of-plane HOMO and LUMO+1 are represented by the pure (p_z–p_z) π MOs, whereas the in-plane HOMO–1 and LUMO are represented mainly by (p_y–p_y) π MOs with a slight contribution from the antibonding σ* (Si–Si) orbital of the central bond. In accordance with the triple-bond structure, a natural bond orbital analysis of **2** shows electron occupation of the two π (Si≡Si) orbitals (1.934 and 1.897 electron), indicating their bonding character. The bond order (Wiberg bond index) of Si1≡Si1' is 2.618, which agrees with the real Si≡Si triple bond [9,16].

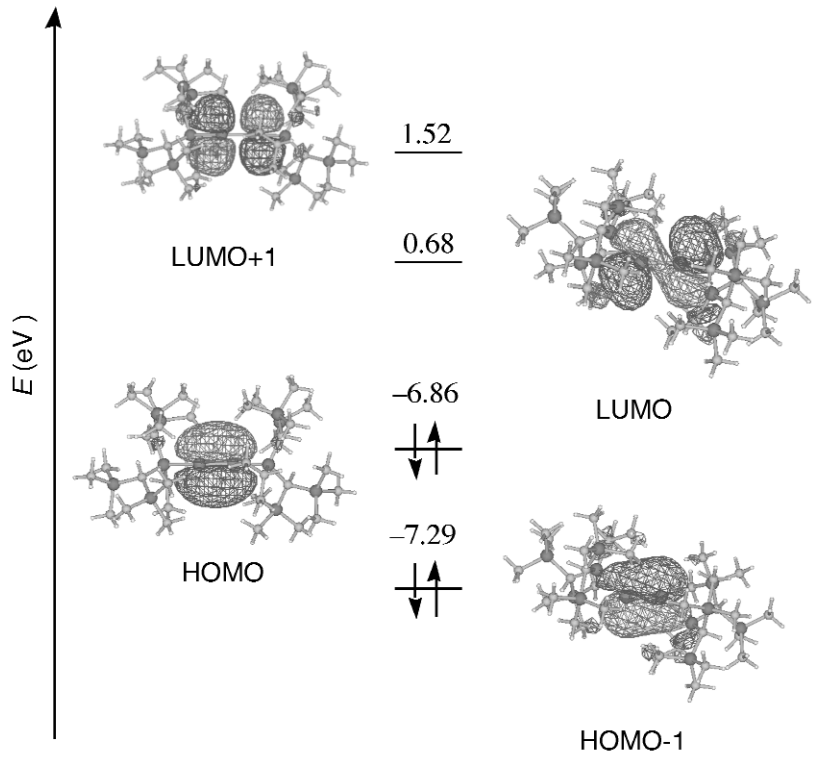

Fig. 4 Molecular orbitals of disilyne **2** calculated at the HF/6-311G(d)//B3LYP/6-31G(d) level.

REACTIVITY OF A DISILYNE

Disilyne has a characteristic structure, and the geometry around the silicon–silicon triple bond is not linear, but *trans*-bent, which results in splitting of the two occupied MOs (π_{in} for HOMO–1 and π_{out} for HOMO) and splitting of the two unoccupied MOs (π^*_{in} for LUMO and π^*_{out} for LUMO+1) [9,15]. Upon bending, the energy of the HOMO is raised, whereas the energy of the LUMO is significantly lowered. Therefore, it is expected that disilyne **2** is prone to easy reduction of its low-lying LUMO. Indeed, the anion radical of disilyne **2** was obtained by one-electron reduction with alkali metals. Thus, the reaction of disilyne **2** with an equivalent amount of lithium, sodium, and KC_8 or potassium metal in THF produced the disilyne anion radicals **3a–c** (Scheme 2). In particular, the potassium salt of disilyne anion radical **3c** was isolated by recrystallization from pentane and 1,2-dimethoxyethane (DME) as dark brown crystals in 63 % isolated yield [17].

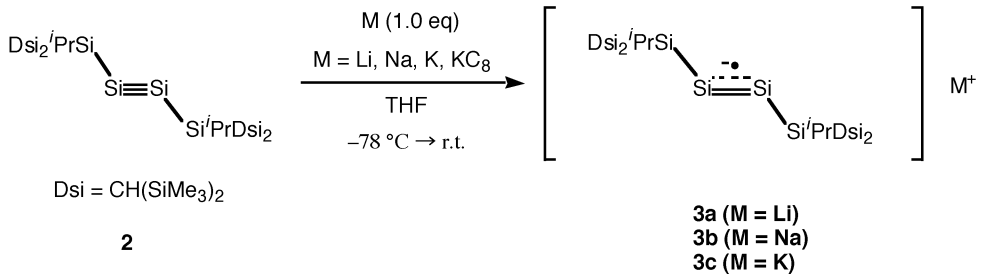

Scheme 2

The electron paramagnetic resonance (EPR) spectra of **3a–c** showed the same signal, indicating that **3a–c** are metal-free disilyne anion radical species [18]. Figure 5 shows the EPR spectrum of **3c** in 2-methyl-THF solvent. The triplet splitting of the signal arises from coupling with the two δ-Hs of the isopropyl groups. The signal is accompanied by two pairs of satellite signals (3.92 and 2.24 mT), due to coupling of the unpaired electron with the α- and β-^{29}Si nuclei, respectively. The magnitude of the spin coupling by the α-^{29}Si nuclei is smaller than that in the tris(di-*tert*-butylmethylsilyl)silyl radical (5.80 mT) [19], implying delocalization of the unpaired electron between the central silicon atoms. The EPR spectra of **3a–c** were also measured in 2-methyl-THF under glass matrix conditions (100 K). As expected, the low symmetry of the disilyne anion radicals **3a–c** caused anisotropy of the *g*-factor, g_{xx} = 2.00907, g_{yy} = 2.00340, g_{zz} = 2.198763.

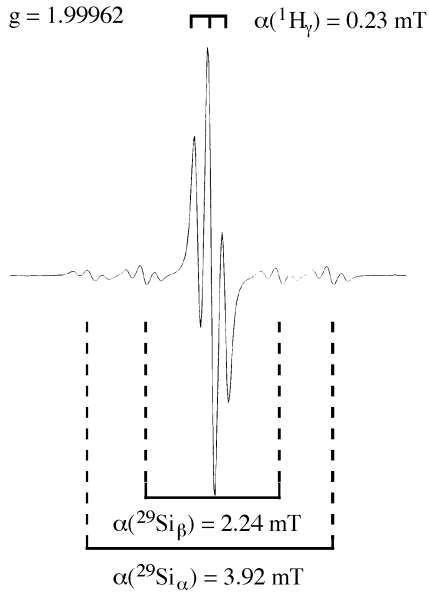

Fig. 5 The EPR spectrum of anion radical **3c** in 2-Me-THF at ambient temperature.

X-ray crystallography unambiguously showed the *trans*-bent structure of disilyne anion radical **3c** (Fig. 6) [17]. The counter cation, potassium, is solvated by four DME molecules and the distance between Si1 and K1 is greater than 11 Å, showing that anion radical **3c** is free. The central Si–Si bond length is 2.1728(14) Å, which is 5 % longer than that of disilyne **2** [2.0622(9) Å] [9] because of the half-occupied π_{in}* orbital with antibonding character. The bond lengths of Si1–Si3 and Si2–Si4 are

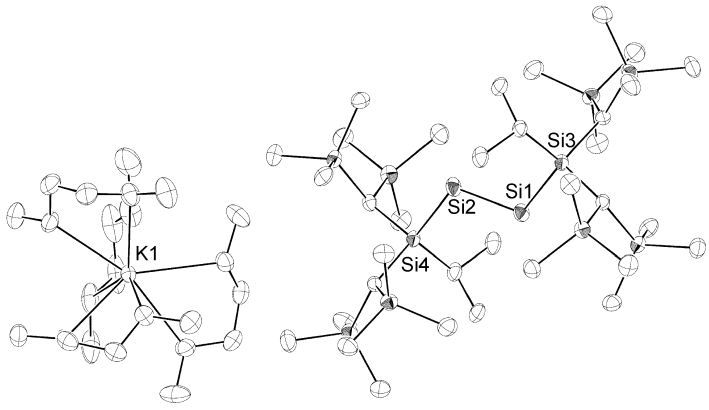

Fig. 6 ORTEP drawing of disilyne anion radical **3c**.

2.3639(13) Å and 2.3714(13) Å, respectively. The characteristic bond angles [112.84(6) and 113.97(6)º] of the tetrasilane unit are smaller than the corresponding bond angle (137.44º) of **2** due to the influence of the negative charge on the central silicon atoms. These bond angles are found to be essentially equal to each other, indicating delocalization of the unpaired electron between the two central silicon atoms.

The reaction of disilyne **2** with an equivalent amount of ^{t}BuLi in dry THF at –78 °C resulted in the immediate development of a red color. Disilenyllithium **4** was isolated as air- and moisture-sensitive red crystals in 82 % isolated yield (Scheme 3) [17]. The disilenide ion was also obtained as a solvent-separated ion pair **5** by the addition of DME to **4**, and purified by recrystallization from pentane, benzene, and DME at –30 °C. The present method provides an entirely new method for the preparation of disilenide derivatives by taking advantage of the reactivity of the silicon–silicon triple bond. The formation of **4** can be rationalized by assuming an initial single-electron transfer process involving intermediate formation of the anion radical of **3a** and *tert*-butyl radical as a key radical pair, followed by fast hydrogen abstraction by the anion radical of **3** with the formation of disilenyllithium [20]. Therefore, disilenyllithium **4** is the product of a formal 1,2-addition of lithium hydride across the Si≡Si triple bond of **2**.

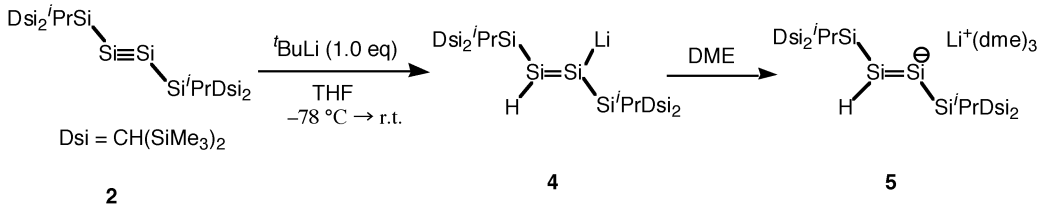

Scheme 3

REACTIVITY OF A DISILYNE TOWARD THE π BOND

To understand the nature of the π bond of a silicon–silicon triple bond, we have examined the reaction of disilyne **2** with alkenes and alkynes. When a hexane solution of disilyne **2** was treated with an excess of *cis*-2-butene at room temperature, *cis*-3,4-dimethyl-1,2-disilacyclobutene **6a** was obtained as the sole product in 89 % yield (Scheme 4) [21]. This reaction proceeded cleanly and was complete within 30 min. On the other hand, the reaction of **2** with *trans*-2-butene under the same conditions produced *trans*-3,4-dimethyl-1,2-disilacyclobutene **6b** as yellow crystals in 85 % yield [21]. In contrast to the reaction with *cis*-2-butene, it took one day to complete this reaction.

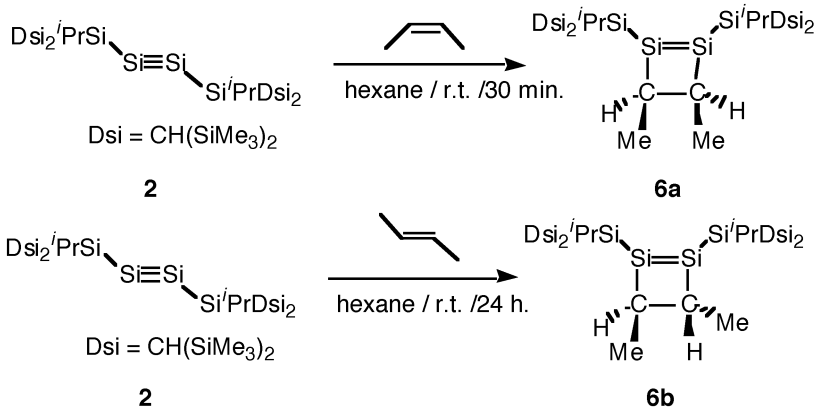

Scheme 4

In order to gain a mechanistic insight, we have performed theoretical calculations of the real system on the reaction of disilyne **2** with 2-butenes. Figure 7 shows the energy profile along the reaction path calculated at the B3LYP/[Si:6-311+G(2df), C and H:6-31G(d)]//B3LYP/3-21G* level. The interaction between the in-plane LUMO (π_{in}*) of **2** and the HOMO of 2-butene, resulting in a formal [1+2] cycloaddition, is the first step in both reactions to produce the silacyclopropyl–silylene intermediate (**Int1**). The alternative interaction between the out-of-plane HOMO (π_{out}) of **2** and the LUMO of 2-butene is unfavorable because of the larger steric repulsion between 2-butene and the $Si^iPr[CH(SiMe_3)_2]_2$ group of **2**. Because the first step is rate-determining, the reaction with *trans*-2-butene, which has a higher energy barrier (ΔE = +23.2 kcal mol^{-1}), requires a longer reaction time than the reaction with *cis*-2-butene (ΔE = +18.4 kcal mol^{-1}). The difference in the heights of the energy barriers is attributed to the degree of steric repulsion between the Me group of 2-butene and the $Si^iPr[CH(SiMe_3)_2]_2$ group of **2**. Finally, the intramolecular insertion of the silylene into the neighboring Si–C bond, followed by rotation about the Si–Si bond with retention of the stereoconfiguration, completes the formation of products **6a**,**b**.

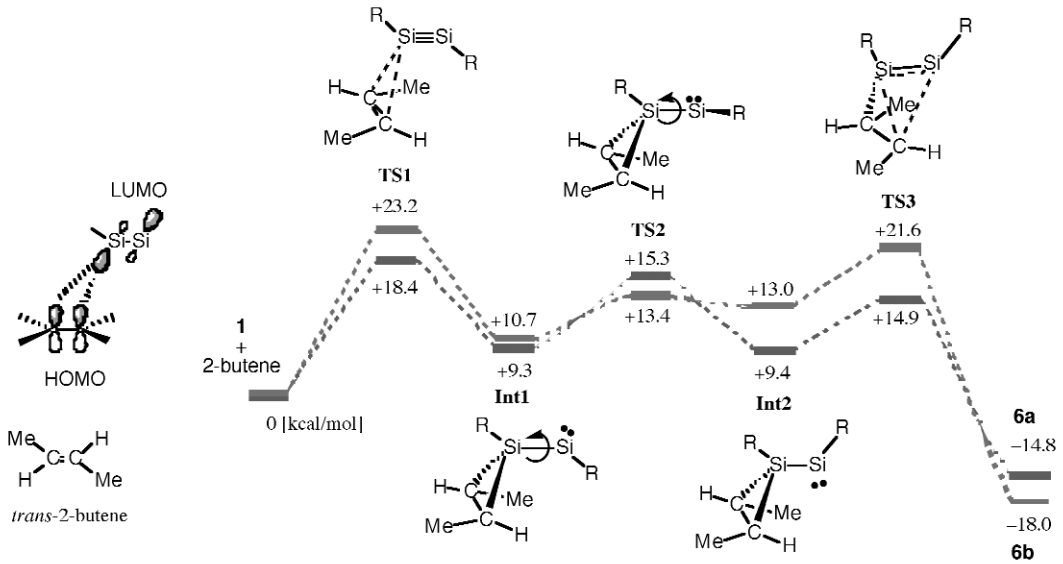

Fig. 7 Calculated energies of transition state and intermediates (kcal mol^{-1}, B3LYP/6-31G).

When a hexane solution of **2** was treated with an excess of phenylacetylene at room temperature, the 1,2-disilabenzene derivative **7** was obtained as a mixture of two regioisomers (**7a**:**7b** = 2:3), isolated as yellow crystals in 63 % overall yield (Scheme 5) [21]. The steric factor is important for the reaction, and no reaction occurred with diphenylacetylene. This is the first example of stable 1,2-disilabenzene derivatives, although the isolation of some stable monosilaaromatic compounds [22], as well as the chemical trapping of intermediary 1,4-disilabenzene and its observation by UV–vis spectroscopy in an Ar matrix at 10 K [23], have already been reported.

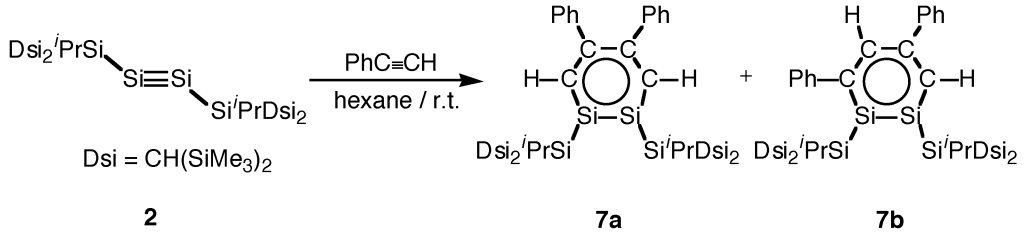

2 **7a** **7b**

Scheme 5

The 1,2-disilabenzene ring of **7a** is almost planar, the sum of the bond angles around the two skeletal Si atoms being 359.74 and 359.83º for Si1 and Si2, respectively (Fig. 8). The dihedral angle between the 1,2-disilabenzene ring and each phenyl group is about 54º. The length of the Si1–Si2 bond is 2.2018(18) Å, which is intermediate between the Si–Si single- and double-bond lengths [16]. The lengths of Si1–C6 and Si2–C3 were found to be essentially equal to each other [1.804(4) and 1.799(5) Å, respectively], and they are intermediate between those of Si–C single- and double-bond lengths. Furthermore, the C3–C4 and C5–C6 bond lengths, which are also equal to each other [1.389(6) and 1.386(6) Å, respectively], are similar to the C–C bond length of the benzene ring (1.39–1.40 Å). The C4–C5 bond length of 1.452(6) Å is different from that of the C–C bond length in the benzene ring, but is intermediate between those of C–C single- and double-bond lengths (1.54 and 1.34 Å, respectively). Thus, it has been experimentally demonstrated that 1,2-disilabenzene has some contribution from the 6π aromatic delocalization, similar to the cases of benzene and monosilabenzene [22,24]. Indeed, nucleus-independent chemical shift (NICS) values, recognized as an aromaticity probe, were calculated for the model compounds **7a'** and **7b'** (Me_3Si groups instead of Si^iPrDsi_2) at 1 Å above the center of the ring: NICS(1) = −8.0 for **7a'** and −8.1 for **7b'** (cf. NICS(1) for benzene = −10.6 [25]).

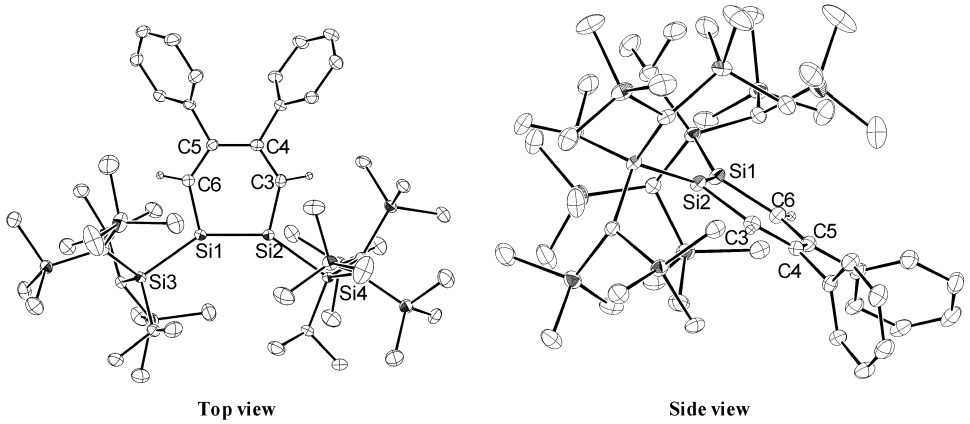

Top view **Side view**

Fig. 8 ORTEP drawing of 1,2-disilabenzene **7a**.

According to the theoretical calculation, the first step in the formation of 1,2-disilabenzene is the generation of a 1,2-disilacyclobutadiene-like intermediate. Then, the [2+4] cycloaddition reaction between this intermediate and a second acetylene molecule will take place to give 1,2-disila-Dewar benzene, followed by its valence isomerization to form the final 1,2-disilabenzene [21].

The MOs of 1,2-disilabenzene **7a** calculated at the HF/6-31G(d) level for X-ray data presented in Fig. 9 show two nondegenerate highest occupied π MOs (HOMO–1 **B** and HOMO **C**) and two lowest unoccupied antibonding π* MOs (LUMO **D** and LUMO+1 **E**). These MOs correspond to those of benzene, although the energy levels are very different. The UV–vis spectrum of **7a** in hexane at room temperature shows two characteristic absorption bands at 427 (116) and 382 (240) nm in the visible region and two broad absorption bands at 313 (745) and 246 (2548) nm in the ultraviolet region. As comparison, the UV–vis spectra of benzene, silabenzene, and 1,4-disilabenzene are also depicted in Fig. 10 [23b]. The absorption maxima of 1,2-disilabenzene **7a** in the visible region are very similar to those of 1,4-disilabenzene (λ = 408, 396, 385, 340, and 275 nm), observed in low-temperature matrices at 10 K. Thus, disilabenzene derivatives showed the remarkable red-shifts as compared with those of benzene, due to the small HOMO-LUMO energy gap (Fig. 9).

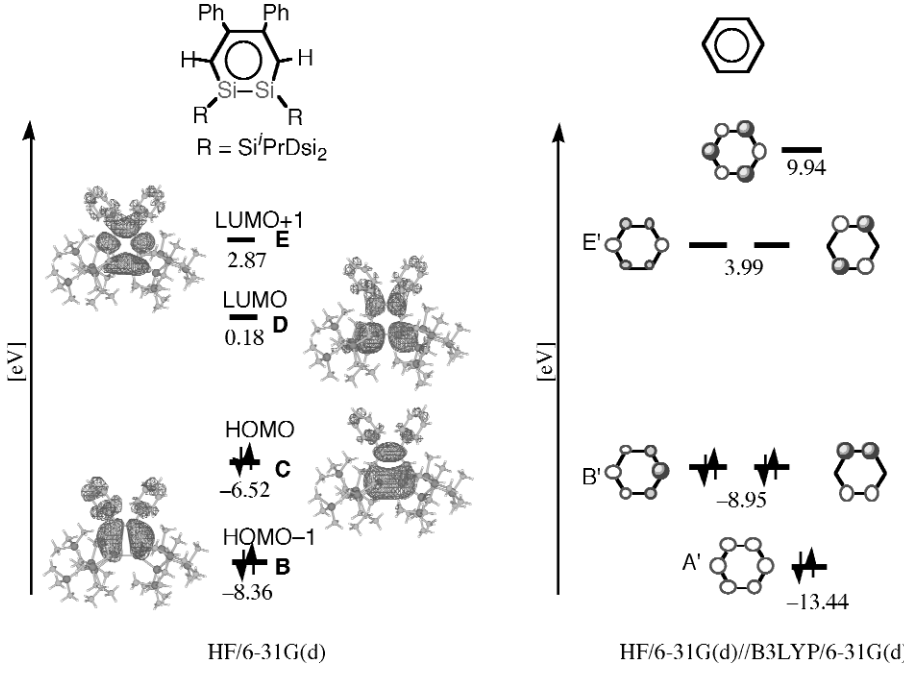

Fig. 9 left: MOs of 1,2-disilabenzene **7a** calculated at the HF/6-31G(d)// level (X-ray data). right: Benzene at the HF/6-31G(d)//B3LYP/6-31G(d) level.

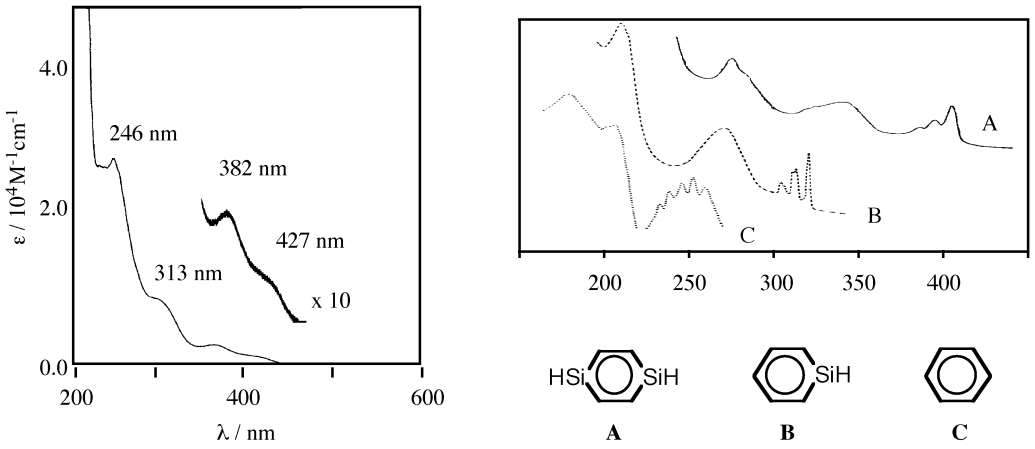

Fig. 10 left: UV–vis spectrum of 1,2-disilabenzene **7a** in hexane at room temperature. right: UV–vis spectra of 1,4-disilabenzene, monosilabenzene, and benzene in Ar matrices at 10 K.

ACKNOWLEDGMENTS

We are highly appreciative of the invaluable experimental contributions by Dr. Rei Kinjo and Dr. Masaaki Ichinohe. We wish to thank Prof. Shigeru Nagase and Dr. Nozomi Takagi for the theoretical calculations. This work was supported by a Grant-in-Aid for Scientific Research (Nos. 19105001, 19020012, 19022004, 19029006) from the Ministry of Education, Science, Sports, and Culture of Japan.

REFERENCES

1. Reviews on double bond chemistry of heavier group 14 elements: (a) P. P. Power. *Chem. Rev.* **99**, 3463 (1999); (b) M. Weidenbruch. *Eur. J. Inorg. Chem.* 373 (1999); (c) J. Escudié, H. Ranaivonjatovo. *Adv. Organomet. Chem.* **44**, 113 (1999); (d) M. Weidenbruch. *The Chemistry of Organic Silicon Compounds*, Vol. 3, Z. Rappoport, Y. Apeloig (Eds.), Chap. 5, John Wiley, Chichester (2001); (e) K. Klinkhammer. *The Chemistry of Organic Germanium, Tin and Lead Compounds*, Vol. 2, Z. Rappoport (Ed.), Part 1, Chap. 4, John Wiley, Chichester (2002); (f) N. Tokitoh, R. Okazaki. *The Chemistry of Organic Germanium, Tin and Lead Compounds*, Vol. 2, Z. Rappoport (Ed.), Part 1, Chap. 13, John Wiley, Chichester (2002); (g) M. Weidenbruch. *Organometallics* **22**, 4348 (2003); (h) V. Ya. Lee, A. Sekiguchi. *Organometallics* **23**, 2822 (2004).
2. P. J. Davidson, M. F. Lappert. *J. Chem. Soc., Chem. Commun.* 317 (1973).
3. R. West, M. J. Fink, J. Michl. *Science* **214**, 1343 (1981).
4. A. G. Brook, F. Abdesaken, B. Gutekunst, G. Gutekunst, R. K. Kallury. *J. Chem. Soc., Chem. Commun.* 191 (1981).
5. Recent reviews on triple bond chemistry of heavier group 14 elements: (a) P. P. Power. *Chem. Rev.* **99**, 3463 (1999); (b) M. Weidenbruch. *J. Organomet. Chem.* **646**, 39 (2002); (c) P. P. Power. *Chem. Commun.* 2091 (2003); (d) M. Weidenbruch. *Angew. Chem., Int. Ed.* **43**, 2 (2004); (e) P. P. Power. *Appl. Organomet. Chem.* **19**, 488 (2005); (f) P. P. Power. *Organometallics* **26**, 4362 (2007).
6. L. Pu, B. Twamley, P. P. Power. *J. Am. Chem. Soc.* **122**, 3524 (2000).
7. M. Stender, A. D. Phillips, R. J. Wright, P. P. Power. *Angew. Chem., Int. Ed.* **41**, 1785 (2002).

8. (a) A. D. Phillips, R. J. Wright, M. M. Olmstead, P. P. Power. *J. Am. Chem. Soc.* **124**, 5930 (2002); (b) Y. Sugiyama, T. Sasamori, Y. Hosoi, Y. Furukawa, N. Takagi, S. Nagase, N. Tokitoh. *J. Am. Chem. Soc.* **128**, 1023 (2006).
9. A. Sekiguchi, R. Kinjo, M. Ichinohe. *Science* **305**, 1755 (2004).
10. N. Wiberg, S. K. Vasisht, G. Fischer, P. Mayer. *Z. Anorg. Allg. Chem.* **630**, 1823 (2004).
11. A. Sekiguchi, M. Ichinohe, R. Kinjo. *Bull. Chem. Soc. Jpn*. **79**, 825 (2006).
12. (a) S. Nagase, K. Kobayashi, N. Takagi. *J. Organomet. Chem.* **611**, 264 (2000); (b) K. Kobayashi, N. Takagi, S. Nagase. *Oraganometallics* **20**, 234 (2001); (c) N. Takagi, S. Nagase. *Chem. Lett.* 966 (2001).
13. M. Ichinohe, M. Toyoshima, R. Kinjo, A. Sekiguchi. *J. Am. Chem. Soc.* **125**, 13328 (2003).
14. N. Takagi, S. Nagase. *Eur. J. Inorg. Chem.* 2775 (2002).
15. A solid-state ^{29}Si NMR study of **2** also supports the presence of two different π-bonds: V. Kravchenko, R. Kinjo, A. Sekiguchi, M. Ichinohe, R. West, Y. S. Balazs, A. Schmidt, M. Karni, Y. Apeloig. *J. Am. Chem. Soc*. **128**, 14472 (2006).
16. G. Frenking, A. Krapp, S. Nagase, N. Takagi, A. Sekiguchi. *ChemPhysChem* **7**, 799 (2006).
17. R. Kinjo, M. Ichinohe, A. Sekiguchi, *J. Am. Chem. Soc*. **129**, 26 (2007).
18. Anion radicals of the alkyne analogs of Ge and Sn: L. Pu, A. D. Phillips, A. F. Richards, M. Stender, R. S. Simons, M. M. Olmstead, P. P. Power. *J. Am. Chem. Soc.* **125**, 11626 (2003).
19. (a) A. Sekiguchi, T. Fukawa, M. Nakamoto, V. Ya. Lee, M. Ichinohe. *J. Am. Chem. Soc.* **124**, 9865 (2002); (b) V. Ya. Lee, A. Sekiguchi. *Eur. J. Inorg. Chem.* 1209 (2005).
20. Disilenides: (a) D. Scheschkewitz. *Angew. Chem., Int. Ed.* **43**, 2965 (2004); (b) M. Ichinohe, K. Sanuki, S. Inoue, A. Sekiguchi. *Organometallics* **23**, 3088 (2004); (c) S. Inoue, M. Ichinohe, A. Sekiguchi. *Chem. Lett.* **34**, 1564 (2005).
21. R. Kinjo, M. Ichinohe, A. Sekiguchi, N. Takagi, M. Sumimoto, S. Nagase. *J. Am. Chem. Soc.* **129**, 7766 (2007).
22. For recent reviews on stable silaaromatic compounds: (a) N. Tokitoh. *Acc. Chem. Res.* **37**, 86 (2004); (b) N. Tokitoh. *Bull. Chem. Soc. Jpn.* **77**, 429 (2004); (c) V. Ya. Lee, A. Sekiguchi. *Angew. Chem., Int. Ed.* **46**, 6596 (2007).
23. (a) J. D. Rich, R. West. *J. Am. Chem. Soc.* **104**, 6884 (1982); (b) G. Maier, K. Schöttler, H. P. Reisenauer. *Tetrahedron Lett.* **26**, 4039 (1985); (c) Y. Kabe, K. Ohkubo, H. Ishikawa, W. Ando. *J. Am. Chem. Soc.* **122**, 3775 (2000).
24. (a) K. Wakita, N. Tokitoh, R. Okazaki, S. Nagase. *Angew. Chem., Int. Ed.* **39**, 634 (2000); (b) K. Wakita, N. Tokitoh, R. Okazaki, N. Takagi, S. Nagase. *J. Am. Chem. Soc.* **122**, 5648 (2000).
25. P. v. R. Schleyer, M. Manoharan, Z.-X. Wang, B. Kiran, H. Jiao, R. Puchta, N. J. R. v. E. Hommes. *Org. Lett*. **3**, 2465 (2001).